

Measurement of the Coupling Strength of Higgs to Vector Bosons in $H \rightarrow WW \rightarrow \ell\nu\ell\nu$ final state with the ATLAS detector at the LHC

Hee Yeun Kim¹

University of Texas at Arlington, 701 S. Nedderman Drive, Arlington, TX 76019, USA

for the ATLAS Collaboration¹

Abstract

We present the measurement of the coupling strength of the Higgs boson to the two vector bosons in the $H \rightarrow WW \rightarrow \ell\nu\ell\nu$ channel. Results using the 25 fb^{-1} of data collected in 7 and 8 TeV center of mass energy by the ATLAS experiment at the LHC are presented [1]. In particular, the extractions of the signal yields from the combination of two major production modes - the gluon-gluon fusion (ggF) and the vector boson fusion (VBF) - and their signal strength correlations are presented. The interpretation of these results with respect to the Standard Model (SM) predictions is also presented.

Keywords: Higgs, $H \rightarrow WW \rightarrow \ell\nu\ell\nu$, LHC, Standard Model, signal strength, Coupling measurement

1. Introduction

The $H \rightarrow WW \rightarrow \ell\nu\ell\nu$ ($l = e, \mu$) channel has advantages for Higgs boson property measurements due to the large signal yield which provides good statistical power to measure the cross section precisely at the Higgs mass $m_H = 125$. Moreover, this channel has direct sensitivity to the Higgs coupling to W bosons and indirect sensitivity to $t\bar{t}H$ coupling via the quantum loop in the ggF production. These characteristics are beneficial for the precision study of SM Higgs properties. The $H \rightarrow WW \rightarrow \ell\nu\ell\nu$ analysis is sensitive to the two ggF and VBF production modes, with the relative sensitivity which depends on the associated jet multiplicity (N_{jet}). The dominant backgrounds depend also on the jet multiplicity: when $N_{\text{jet}} \leq 1$, the WW and the top background are dominant while the top background is the most dominant for $N_{\text{jet}} \geq 2$. Fig. 1 shows the N_{jet} distribution after the pre-selection and $E_{T,\text{rel}}^{\text{miss}}$ cut in the different lepton flavor composition ($e\mu + \mu e$) where $E_{T,\text{rel}}^{\text{miss}}$

is defined as $E_T^{\text{miss}} \times \sin \Delta\Phi_{\ell\ell}$ (for $\Delta\Phi_{\ell\ell} < \frac{\pi}{2}$, otherwise E_T^{miss}).

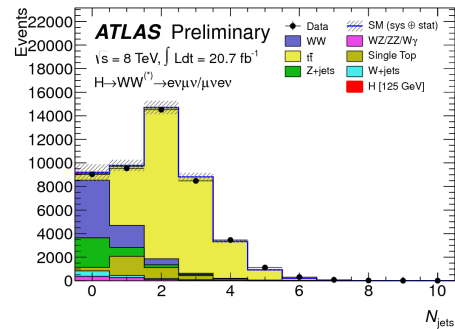


Figure 1: N_{jet} distribution after pre-selection and $E_{T,\text{rel}}^{\text{miss}}$ for $e\mu + \mu e$ [3]

2. Event selection

With respect to the previous analysis [2], which considered only different lepton flavor composition ($e\mu + \mu e$) in the final state, the present analysis adds the same flavor lepton composition ($\mu\mu + ee$). $N_{\text{jet}} \geq 2$ is added to

Email address: hee.yeun.kim@cern.ch (Hee Yeun Kim)

the present study to increase the sensitivity to the VBF production mode. Exactly two opposite-charged leptons (e, μ) in any flavor combinations are selected and are required to pass stringent identification criteria in addition to isolation requirements. The leading lepton is required to have a $p_T^{\text{lead}} \geq 25 \text{ GeV}$ while sub-leading $p_T^{\text{sublead}} > 15 \text{ GeV}$ and $|\eta| < 1.37$ and $1.52 < |\eta| < 2.47$ for electrons while $|\eta| < 2.5$ is for the muon.

Jets are reconstructed using the anti- k_T algorithm with distance parameter $\Delta R=0.4$, and the number of jets identified by a b-tagging algorithm ($N_{b\text{-jet}}$) are used to veto jets initiated by a b quark for $N_{\text{jet}} \geq 1$. The Drell-Yan (DY) and multi-jet backgrounds are suppressed by requiring large $E_{T,\text{rel}}^{\text{miss}}$. A signal region (SR) and a control region (CR) are defined by the $m_{\ell\ell}$ and $\Delta\Phi_{\ell\ell}$ which are the invariant mass and $\Delta\Phi$ of the di-lepton system, respectively. The transverse mass m_T is used in the final fit and is defined as $m_T = \sqrt{((E_T^{\ell\ell} + E_T^{\text{miss}})^2 - |P_T^{\ell\ell} + E_T^{\text{miss}}|^2)}$ with $E_T^{\ell\ell} = \sqrt{(|P_T^{\ell\ell}|^2 + m_{\ell\ell}^2)}$. The signal lies mainly around in $90 < m_T < 125 \text{ GeV}$ range. More details of the event selection can be found in Ref. [3].

3. Background estimation

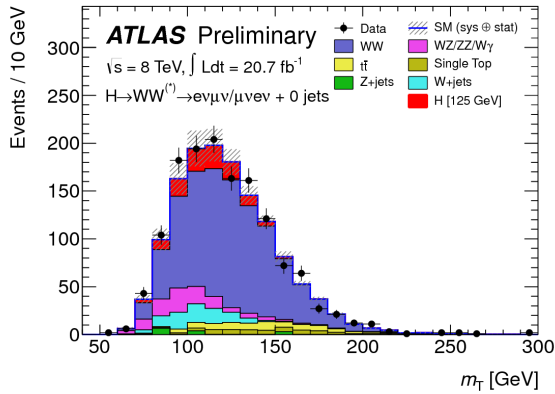


Figure 2: Distribution of the m_T for 8 TeV data for $e\mu+\mu e$ when $N_{\text{jet}} = 0$ [3]

3.1. WW Background

The WW process is the most dominant background for $N_{\text{jet}} = 0$. Figure 2 shows the expected signal and the composition of the expected background for $e\mu+\mu e$ in the $N_{\text{jet}} = 0$ and the WW background is the major background in this category. It is also comparable to the single top yield for in $N_{\text{jet}} = 1$ and is a small but still significant contribution for the $N_{\text{jet}} \geq 2$ channel. The predicted distributions of the WW background in $N_{\text{jet}} =$

0 and $N_{\text{jet}} = 1$ are normalized using a WW enriched orthogonal CR while it is estimated from simulation for the $N_{\text{jet}} \geq 2$ channel. The CR is defined as $50 \leq m_{\ell\ell} \leq 100 \text{ GeV}$ and $m_{\ell\ell} > 80 \text{ GeV}$ for $N_{\text{jet}} = 0$ and 1, respectively. The normalization factors (NF) are 1.16 ± 0.04 (stat.) for $N_{\text{jet}} = 0$ and 1.03 ± 0.06 (stat.) for $N_{\text{jet}} = 1$. The total uncertainty on the WW background is 7.4%, 37%, and 37% for the $N_{\text{jet}} = 0, = 1,$ and ≥ 2 modes, respectively.

3.2. Top Background

The top background in the $N_{\text{jet}} = 0$ bin is estimated using inclusive-jet top-dominated data, multiplied by the simulated fraction of top events without reconstructed jets from that by a b-tagged jets are removed [2]. For the $N_{\text{jet}} = 1$ bin and ≥ 2 jet bin, the top background is normalized in the CR requiring one b-tagged jet and removing the $\Delta\Phi_{\ell\ell}$ and $\Delta m_{\ell\ell}$ requirements.

3.3. W+jet and non-WW Diboson Background

The W+jets background shape and normalization are estimated from data. The W+jets background in SR is obtained by scaling the number of events in the data CR by the fake factor (FF) that is defined as the ratio of the number of lepton candidates passing all selections to the ones failing to pass the selections. The total fake factor uncertainty is 45% (40%) for mis-identified electrons (muons). Simulation is used to estimate the non-WW diboson background and the uncertainties in the SR are 16% ($N_{\text{jet}} = 0$) and 22% ($N_{\text{jet}} = 1$).

4. Systematic uncertainties

The systematic uncertainties are divided into two categories: experimental and theoretical. QCD renormalization and factorization scale uncertainties affect the prediction of ggF signal and are also the main source of uncertainty on the WW background. In addition, the uncertainties from Parton Showering scheme (PS) and the Underlying Events (UE) are non-negligible. The experimental uncertainty is dominated by final object (leptons, jets, and E_T^{miss}) selection and energy/momentum scale and resolution of the different objects.

5. Result

The observed significance of the signal with $m_H = 125 \text{ GeV}$ is 3.8σ (Exp. 3.7σ), but the highest significance, 4.1σ , is found at $m_H = 140 \text{ GeV}$. The signal strength ($\hat{\mu}$) of 7 and 8 TeV data combining all jet multiplicity is

$$\begin{aligned} \mu_{\text{obs}} &= 1.01 \pm 0.21(\text{stat.}) \pm 0.19(\text{theo.}) \\ &\quad \pm 0.12(\text{expt.}) \pm 0.04(\text{lumi.}) \\ &= 1.01 \pm 0.31(\text{tot.}), \end{aligned}$$

and the observed VBF signal significance at $m_H = 125$ GeV is 2.5σ (Exp. 1.6σ). Statistical tests of the VBF signal are performed on the data by treating the ggF signal as part of the background. The test defines μ_{VBF} , the signal strength parameter associated with the VBF process, as the parameter of interest. The ggF signal strength μ_{ggF} is constrained mainly by the $N_{jet} \leq 1$ signal regions. The best-fit measured signal strength at $m_H = 125$ GeV is

$$\mu_{obs,ggF} = 0.82 \pm 0.36, \quad \mu_{obs,VBF} = 1.66 \pm 0.79$$

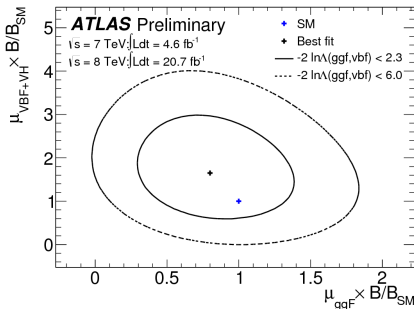


Figure 3: Likelihood contours and best-fit value [3]

Figure 3 shows a two-dimensional likelihood scan of the signal strength for the ggF and VBF production modes and the best fit lies within 1σ range of Standard Model expectation (denoted as the blue +). The cross section measured with 8 TeV data at $m_H = 125$ GeV is [3]

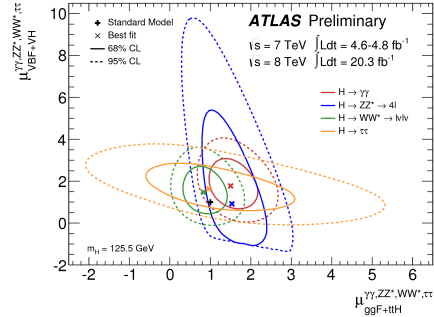
$$(\sigma \cdot B) = 6.0 \pm 1.6 \text{ pb (Exp. } 4.8 \pm 0.7 \text{ pb)}.$$

6. Combined Coupling measurement

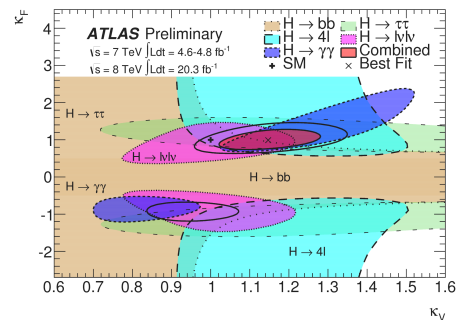
The $H \rightarrow WW \rightarrow \ell\nu\ell\nu$ channel has been combined with other Higgs decay channels [4] and the measured combined mass is 125.5 GeV. Fig. 4a shows the likelihood contours in the μ_{ggF+iH} and μ_{VBF+VH} plane at $m_H = 125.5$ GeV. The total combined signal strength is $\mu = 1.30 \pm 0.12$ (stat.) $^{+0.14}_{-0.11}$ (sys.). The coupling measurement is also done. The measured coupling scale factors are $\kappa_V = 1.15 \pm 0.08$ and $\kappa_F = 0.99^{+0.17}_{-0.15}$ [5]. The correlation of the coupling scale factors κ_V and κ_F overlaying the 68% CL contours derived from the individual channels and their combination is shown in Fig. 4b. From both figures, SM expectation lies within 1σ range of $H \rightarrow WW \rightarrow \ell\nu\ell\nu$ channel.

7. Conclusions

The analysis of the $H \rightarrow WW \rightarrow \ell\nu\ell\nu$ process in the mass range of 115 - 200 GeV is presented using the complete data sample of 2011 and 2012. The signal significance at $m_H = 125$ GeV is 3.8σ and the best fit signal



(a) Likelihood contours in the μ_{ggF+iH} and μ_{VBF+VH} plane



(b) Likelihood contours of coupling scale factors κ_V and κ_F

Figure 4: Results of correlation fits for the 2-parameters in the combination: (a) μ_{ggF+iH} vs. μ_{VBF+VH} , (b) κ_V vs. κ_F [5]

strength at that mass is $\mu = 1.01 \pm 0.31$. The measured value of the product of the cross section and the WW branching ratio for a signal at $m_H = 125$ GeV at 8 TeV is 6.0 ± 1.6 pb while the expected value is 4.8 ± 0.7 pb. The results of the study agree with the prediction of the SM Higgs boson through $H \rightarrow WW \rightarrow \ell\nu\ell\nu$ channel.

References

- [1] ATLAS Collaboration, *The ATLAS Experiment at the CERN Large Hadron Collider*, 2008 JINST 3 S08003.
- [2] ATLAS Collaboration, *Update of the $H \rightarrow WW \rightarrow \ell\nu\ell\nu$ analysis with 13 fb^{-1} of $\sqrt{s} = 8$ data collected with the ATLAS Detector*, ATLAS-CONF-2012-158(2012), <https://cds.cern.ch/record/1493601>.
- [3] ATLAS Collaboration, *Measurements of the properties of the Higgs-like boson in the $WW^* \rightarrow \ell\nu\ell\nu$ decay channel with the ATLAS detector using 25 fb^{-1} of proton-proton collision data*, ATLAS-CONF-2013-030(2013), <https://cds.cern.ch/record/1527126>.
- [4] ATLAS Collaboration, *Measurements of Higgs boson production and couplings in diboson final states with the ATLAS detector at the LHC*, Physics Letters B 726 (2013) 88119.
- [5] ATLAS Collaboration, *Updated coupling measurements of the Higgs boson with the ATLAS detector using up to 25 fb^{-1} of proton-proton collision data*, ATLAS-CONF-2014-009(2014), <https://cds.cern.ch/record/1670012>.